Thermochimica Acta, 185 (1991) 315–333
Elsevier Science Publishers B.V., Amsterdam

Thermal studies of sulphonamide derivative complexes. Part III. Thermal behaviour of acetazolamide complexes of Co(II), Ni(II) and Cu(II) with ethylamine, diethylamine, triethylamine and potassium hydroxide

G. Alzuet [a], S. Ferrer [a], J. Borrás [a,1], J. Martín-Gil [b] and F.J. Martín-Gil [b]

[a] *Dpto. Química Inorgánica, Facultad de Farmacia, Universidad de Valencia, Valencia (Spain)*
[b] *Dpto. Química Inorgánica, ETSII de Valladolid, Universidad de Valladolid, Valladolid (Spain)*

(Received 17 December 1990)

Abstract

A thermal study of a new series of acetazolamidate complexes of Co(II), Ni(II) and Cu(II) using the TG, DTG and DTA techniques in flowing air, static air and N_2 atmospheres is described.

From the TG–DTG and DTA curves, different thermal behaviours can be observed. Although in all the complexes the processes of dehydration, deammination and pyrolysis can be clearly observed, in some cases they appear as several well-separated steps and, in others, as continuous stages which take place simultaneously.

The differences observed between the pyrolytic decomposition in flowing air and in nitrogen are described. In flowing air, metal sulphate is formed from the thiadiazole ring, except for potassium salts in which the sulphate derives from the sulphonamide group. The formation of sulphate from the thiadiazole ring is accompanied by a strong exothermic peak in the DTA curve. In contrast, in nitrogen, metal sulphide nor sulphate is formed.

INTRODUCTION

Acetazolamide (Acm 5-acetamido-1,3,4-thiadiazole-2-sulphonamide) is one of the most potent inhibitors of carbonic anhydrase enzyme. We have initiated studies on the coordination chemistry of Acm with metals ions [1–4]. In previous papers, the thermal behaviour of several Acm complexes has been reported [5,6]. In the present work, as a continuation of this study, we report the thermal decomposition of a new series of Acm complexes obtained by adding potassium hydroxide, ethylamine (EA), diethylamine (DEA) and triethylamine (TEA).

---

[1] Author for correspondence. Dpto. Química Inorgánica, Facultad de Farmacia, Universidad de Valencia, Blasco Ibáñez 13, 46010 Valencia, Spain.

EXPERIMENTAL

Apparatus

TG analyses were performed in air and nitrogen atmospheres using Perkin–Elmer 3600 and DTA 1700 instruments, at a heating rate of 10 °C min^{-1}. Thermolytic reactions were obtained with samples varying in weight from 1 to 8 mg. The TG–DTG and DTA curves are shown from 60 °C but they were registered from 25 °C.

IR spectra were obtained using KBr pellets on a Perkin–Elmer Model 843 spectrophotometer. Reflectance spectra were recorded on a Perkin–Elmer Lambda 15 spectrometer.

Samples

The complexes $(TEAH)_2Co_2(Acm)_3.2H_2O$, $(DEAH)_2Co_2(Acm)_3.1/2H_2O$, $(EAH)_2Co_2(Acm)_3.6H_2O$, $(TEAH)_2Ni_2(Acm)_3.3H_2O$, $(DEAH)_2Ni_2(Acm)_3.3H_2O$, $(EAH)_6Cu_2(Acm)_5.H_2O$, $(DEAH)_2Cu_4(Acm)_5.3H_2O$, $(TEAH)_2Cu_4$-$(Acm)_5.3H_2O$, $K_6Cu_2(Acm)_5.2H_2O$ and $K_6Co(Acm)_4.6H_2O$ were prepared according to the methods previously reported [7].

RESULTS AND DISCUSSION

$R_2Co_2(Acm)_3.nH_2O$

$(EAH)_2Co_2(Acm)_3.6H_2O$

In the first step, the TG–DTG curves of the complex (Fig. 1) show a loss of weight up to 100 °C, corresponding to the elimination of four water molecules. The DTA (Fig. 1) curve exhibits a weak endothermic region in the temperature range at which the dehydration takes place.

In the following step (between 100 and 400 °C), the loss of weight can be assigned to the elimination of the remaining water molecules together with the deammination and the elimination of the sulphonamido and acetamido groups. In the DTA curve, only a broad exothermic peak is observed. No thermal events for the deammination and the dehydration processes are detected; consequently the exothermic peak appears to be a combination of the endothermic removal of amine and H_2O as well as the exothermic pyrolytic decomposition of the ligand.

$(DEAH)_2Co_2(Acm)_3.1/2H_2O$

In the first step, the TG–DTG curves (Fig. 2) show a loss of weight corresponding to one molecule of amine and half a molecule of water between 30 and 90 °C. In the same temperature range, the DTA curve (Fig.

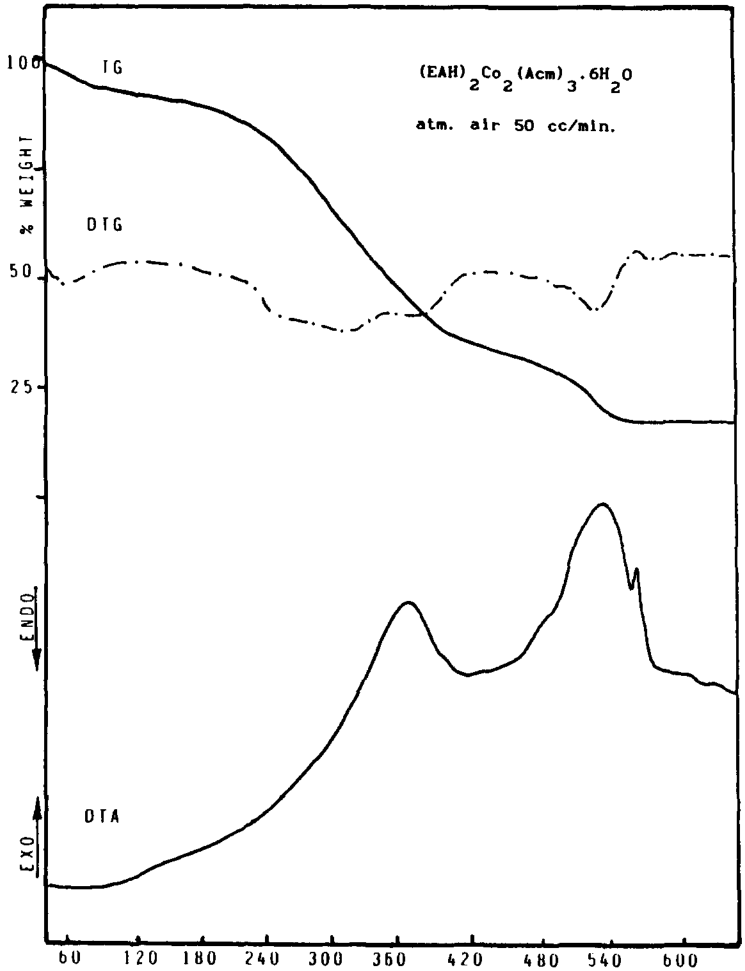

Fig. 1. TG, DTG and DTA thermograms for $(EAH)_2Co_2(Acm)_3.6H_2O$ in dynamic air at 10 °C min^{-1}.

2) exhibits two weak endothermic peaks overlapping with each other, due to deammination and dehydration.

The significant loss of weight up to 390 °C is due to the removal of the remaining amine, together with that of the sulphonamido and acetamido groups. The DTA curve presents a very weak endothermic region with a maximum at 240 °C that can be attributed to deammination, and a strong exothermic peak at 365 °C, characteristic of the ligand degradation.

$(TEAH)_2Co_2(Acm)_3.2H_2O$

The loss of weight observed below 80 °C in the TG–DTG curves (Fig. 3) corresponds to the liberation of two molecules of crystallisation water. In

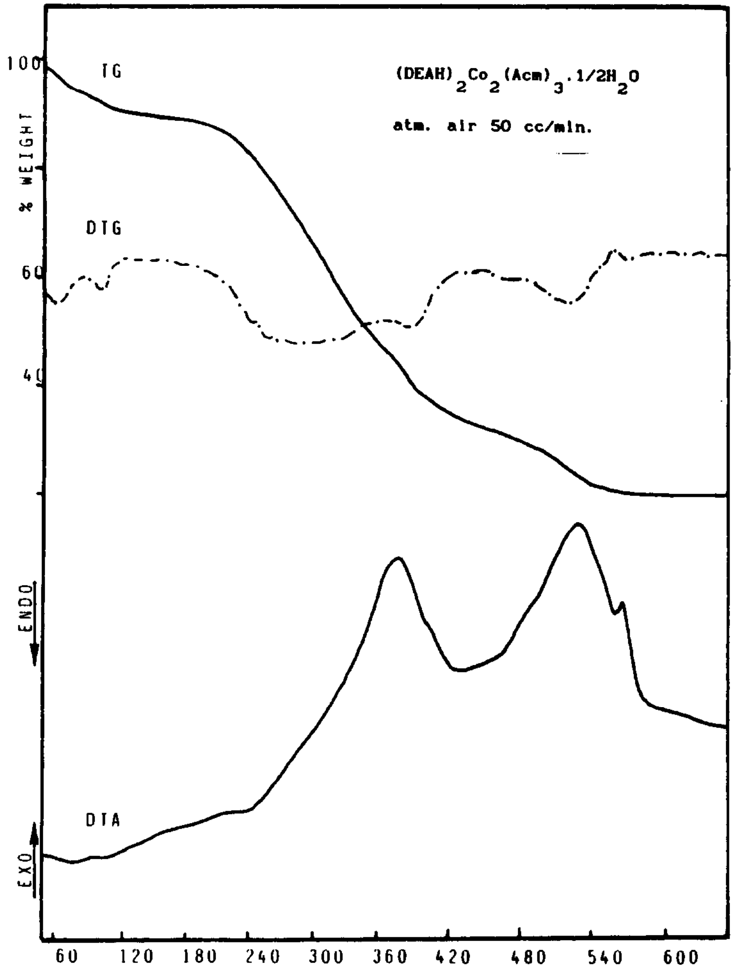

Fig. 2. TG, DTG and DTA thermograms for $(DEAH)_2Co_2(Acm)_3.1/2H_2O$ in dynamic air at 10 °C min^{-1}.

the DTA curve (Fig. 3), the dehydration appears as an endothermic region between 30 and 60 °C.

In the next step (temperature range 190–280 °C), the deammination proceeds simultaneously with the first stage of the pyrolytic degradation of the ligand. The loss of weight at the end of this thermal event corresponds to the elimination of the two molecules of amine and of the three acetamido groups. An endothermic peak followed by an exothermic one, assigned to the same processes, can be observed in the DTA curve.

In the second step of the ligand degradation, which appears inmediately after the first, the sulphonamido groups are lost. The DTA curve exhibits a corresponding exothermic peak with a maximum at 380 °C.

In all of the above-mentioned compounds, the last step of the ligand

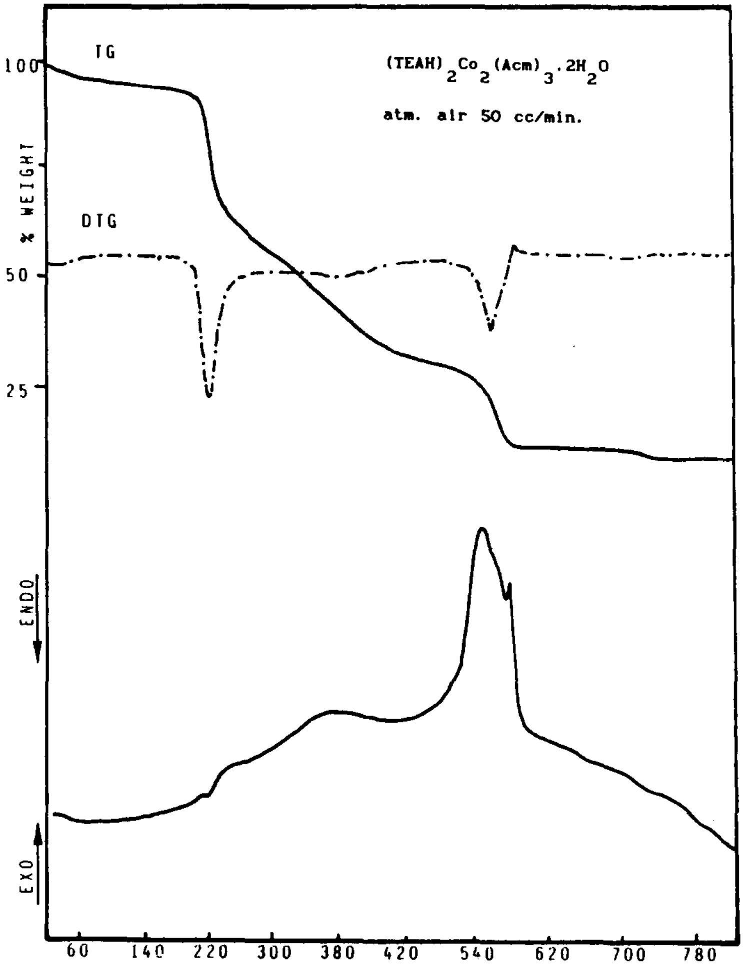

Fig. 3. TG, DTG and DTA thermograms for $(TEAH)_2Co_2(Acm)_3.2H_2O$ in dynamic air at 10 °C min^{-1}.

degradation gives a Co-thiadiazole derivative [6,8]. The formation of the thiadiazole derivative has been confirmed by IR spectroscopy. The IR spectra of the corresponding samples taken at 420 °C are characterised by a broad IR band over 1400 cm^{-1} typical of compounds such as thiadiazole [9,10].

The metal thiadiazole derivative is decomposed by partial oxidation of the sulphur atom of the thiadiazole ring to a mixture of $CoSO_4$ and CoO [6]. The DTG curves at 500 °C for $(EAH)_2Co_2(Acm)_3.6H_2O$ and $(DEAH)_2Co_2(Acm)_3.2H_2O$, and at 590 °C for $(TEAH)_2Co_2(Acm)_3.2H_2O$, suggest that a very small amount of cobalt sulphate is formed. The presence of $CoSO_4$ has been confirmed by IR spectroscopy and is supported by a strong exothermic peak observed in the DTA curve at about 550 °C.

The final residue is CoO.

The following schemes summarise the thermal degradation of these complexes

$$\mathrm{(EAH)_2Co_2(Acm)_3.6H_2O} \xrightarrow[\substack{\text{Exp.: 7.1\%}\\ \text{Calc.: 7.3\%}}]{-4\mathrm{H_2O}} \mathrm{(EAH)_2Co_2(Acm)_3.2H_2O}$$

$$\xrightarrow{-2\mathrm{H_2O},\ -2\mathrm{EA}} \xrightarrow[\substack{\text{Exp.: 55.6\%}\\ \text{Calc.: 55.3\%}}]{-3\mathrm{AcNH_2},\ -3\mathrm{SO_2NH_2}} \mathrm{Co_2[Tdz]_3} \rightarrow \mathrm{CoO} + \mathrm{CoSO_4} \rightarrow 2\mathrm{CoO}$$

(Residue: exp., 16.2%; calc., 15.3%)

$$\mathrm{(DEAH)_2Co_2(Acm)_3.1/2H_2O} \xrightarrow[\substack{\text{Exp.: 9.2\%}\\ \text{Calc.: 8.9\%}}]{-1/2\mathrm{H_2O},\ -\mathrm{DEA}} \mathrm{(DEAH)Co_2(Acm)_3}$$

$$\xrightarrow{-\mathrm{DEA}} \xrightarrow[\substack{\text{Exp.: 54.2\%}\\ \text{Calc.: 52.1\%}}]{-3\mathrm{AcNH_2},\ -3\mathrm{SO_2NH_2}} \mathrm{Co_2[Tdz]_3} \rightarrow \mathrm{CoO} + \mathrm{CoSO_4} \rightarrow 2\mathrm{CoO}$$

(Residue: exp., 16.9%; calc., 16.0%)

$$\mathrm{(TEAH)_2Co_2(Acm)_3.2H_2O} \xrightarrow[\substack{\text{Exp.: 3.5\%}\\ \text{Calc.: 3.5\%}}]{-2\mathrm{H_2O}} \mathrm{(TEAH)_2Co_2(Acm)_3}$$

$$\xrightarrow[\substack{\text{Exp.: 37.7\%}\\ \text{Calc.: 37.1\%}}]{-2\mathrm{TEA},\ -3\mathrm{AcNH_2}} \mathrm{Co_2[Tdz{-}SO_2NH_2]_3} \xrightarrow[\substack{\text{Exp.: 24.3\%}\\ \text{Calc.: 23.5\%}}]{-3\mathrm{SO_2NH_2}} \mathrm{Co_2[Tdz]_3}$$

$\rightarrow \mathrm{CoO} + \mathrm{CoSO_4} \rightarrow 2\mathrm{CoO}$ (Residue: exp., 15.1%; calc., 14.7%)

$(DEAH)_2Ni_2(Acm)_3.3H_2O$ and $(TEAH)_2Ni_2(Acm)_3.3H_2O$

The TG–DTG curves for these complexes are shown in Figs. 4 and 5, respectively. The dehydration takes place up to 100 °C, which means that the water is water of hydration. The DTA curves (Figs. 4 and 5) show the corresponding endothermic region due to the liberation of water.

The deammination process begins at 100 °C for diethylammonium and at 180 °C for triethylammonium. The DTA curve exhibits an endothermic peak in the TEAH salt. However, no thermal event is observed in the DTA curve of the DEAH salt, probably because the corresponding endothermic peak is overlapping with the following exothermic one.

The ligand pyrolysis takes place in two stages. In the first step, the elimination of the sulphonamido and acetamido groups occurs leaving a nickel thiadiazole derivative in both complexes. The formation of these species is also indicated by the IR spectra of the samples taken at about

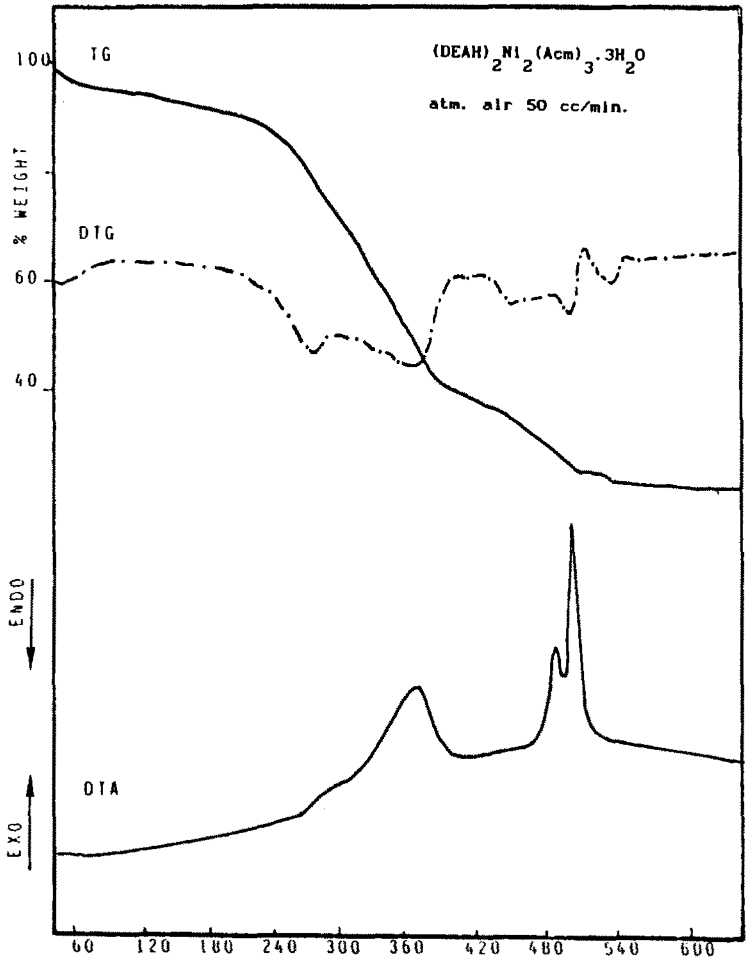

Fig. 4. TG, DTG and DTA thermograms for $(DEAH)_2Ni_2(Acm)_3.3H_2O$ in dynamic air at 10 °C min^{-1}.

400 °C which show a broad band centred over 1400–1500 cm^{-1} and a medium band at 600 cm^{-1}, characteristic of molecules containing S=C=N bonds [9]. An exothermic peak, attributed to the pyrolytic stage, appears in the DTA curves at 365 °C and 310 °C, respectively.

The Ni thiadiazole derivative then gives a mixture of Ni(II) sulphide and Ni(II) sulphate. The presence of sulphate is observed in the DTG curve and confirmed by IR spectroscopy. The NiS decomposes to NiO and the final residue is composed of a mixture of $NiSO_4$ and NiO for $(DEAH)_2Ni_2(Acm)_3$. $3H_2O$ and NiO for $(DEAH)_2Ni_2(Acm)_3.3H_2O$. In the DTA curves the shape of the exothermic peaks attributed to the oxidation processes is different from that of the Co(II) and Cu(II) complexes, which is in agreement with TG–DTG results, discussed above.

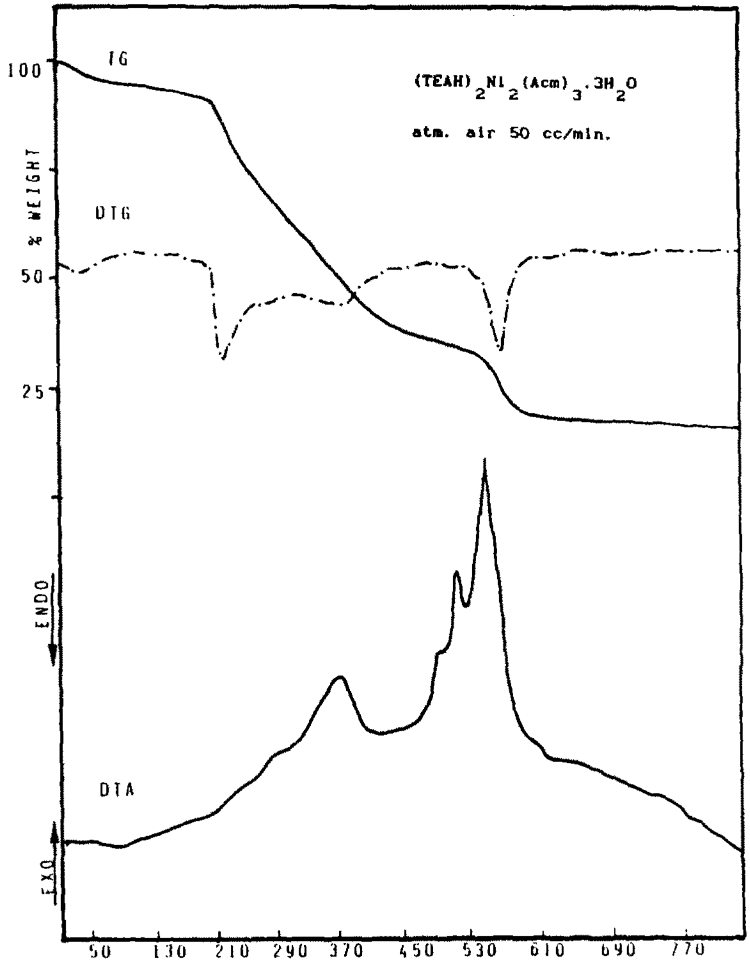

Fig. 5. TG, DTG and DTA thermograms for $(TEAH)_2Ni_2(Acm)_3.3H_2O$ in dynamic air at 10 °C min^{-1}.

The thermal decomposition of the complexes can be summarised as follows

$$(DEAH)_2Ni_2(Acm)_3.3H_2O \xrightarrow[\text{Exp.: 5.3\%}]{-3H_2O} (DEAH)_2Ni_2(Acm)_3$$

Calc.: 5.5%

$$\xrightarrow{-2DEA} \xrightarrow[\text{Exp.: 57.2\%}]{-3AcNH_2,\ -3SO_2NH_2} Ni_2[Tdz]_3 \rightarrow NiO + NiS + NiSO_4$$

Calc.: 57.3%

$$\rightarrow NiO + NiSO_4 \quad \text{(Residue; exp., 21.6\%; calc., 23.1\%)}$$

$$(TEAH)_2Ni_2(Acm)_3.3H_2O \xrightarrow[\text{Exp.: 5.6\%}]{-3H_2O} (TEAH)_2Ni_2(Acm)_3$$

Calc.: 5.1%

$$\xrightarrow[\text{Exp.: 21.1\%}]{-2\text{TEA}} \mathrm{Ni_2(Acm)_3} \xrightarrow[\text{Exp.: 39.4\%}]{-3\text{AcNH}_2,\ -3\text{SO}_2\text{NH}_2} \mathrm{Ni_2[Tdz]_3}$$

Calc.: 19.7% Calc.: 39.9%

$$\rightarrow \mathrm{NiO + NiS + NiSO_4} \rightarrow \mathrm{2NiO}\ \text{(Residue: exp., 14.8\%; calc., 14.4\%)}$$

$R_2Cu_4(Acm)_5.3H_2O$ and $(EAH)_6Cu_2(Acm)_5.H_2O$ (R = DEAH and TEAH)

$(EAH)_6Cu_2(Acm)_5.H_2O$

The TG and DTG curves for $(EAH)_6Cu_2(Acm)_5.H_2O$ are shown in Fig. 6. The dehydration of the complex occurs between 30 and 60 °C which means that water is present as water of crystallisation; this was confirmed by the RD spectrum of the compound after heating at 120 °C. As expected,

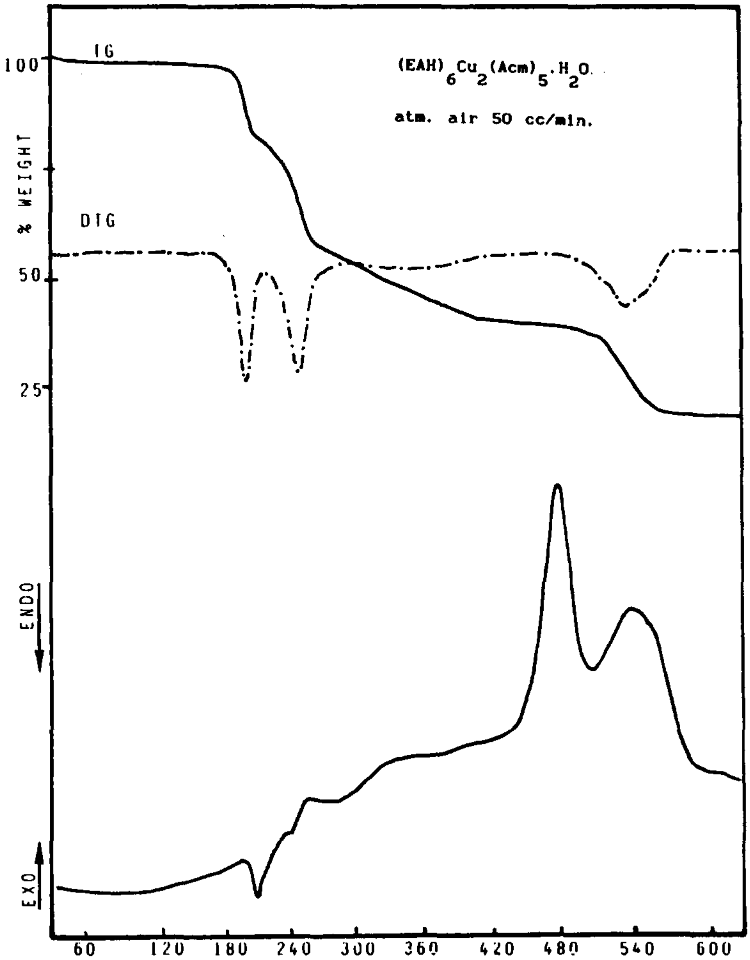

Fig. 6. TG, DTG and DTA thermograms for $(EAH)_6Cu_2(Acm)_5.H_2O$ in dynamic air at 10 °C min^{-1}.

the RD spectrum of the anhydrous complex is almost identical to that of the hydrated compound. The DTA curve (Fig. 6) shows an undefined endothermic region over the same temperature range.

The deammination process takes place in a single step between 180 and 230 ° C. An endothermic peak centred at 200 ° C in the DTA curve accounts for the elimination of the six amine molecules.

The first step of the ligand degradation, which is contiguous with the loss of ethylamine, corresponds to the elimination of sulphonamido groups from the ligand. This thermal event can be observed in the DTA curve as an exothermic peak between 240 and 270 ° C, next to the previous endothermic peak which was attributed to deammination.

The second pyrolytic decomposition step of the ligand, which involves the loss of acetamido groups, occurs between 300 and 400 ° C. In the DTA curve, the process is characterised by an exothermic peak.

$(DEAH)_2Cu_4(Acm)_5.3H_2O$

The TG–DTG curves (Fig. 7) show a first loss of weight between 30 and 100 ° C, corresponding to the removal of two water molecules. The low temperature at which the elimination of these molecules takes place indicates their hydration nature. The nature of the water molecules has been confirmed by the RD spectrum of the anhydrous complex that exhibits the same pattern as that of the hydrated complex. The dehydration of the complex is accompanied by the characteristic endothermic region in the DTA curve (Fig. 7).

The deammination, together with the elimination of the last water molecule, begins at 140 ° C. The loss of water at temperatures higher than in the other complexes already described, suggests that one molecule of water is probably bonded through strong hydrogen bonds in the complex structure [11,12]. The DTA curve exhibits one endothermic peak only due to both processes, centred at 210 ° C. Then, ligand pyrolysis takes place. The loss of weight between 230 and 390 ° C is due to the elimination of the sulphonamido and acetamido groups. The endothermic peak, attributed to this pyrolytic stage, appears in the DTA curve at 360 ° C.

$(TEAH)_2Cu_4(Acm)_5.3H_2O$

As shown in the TG–DTG curves (Fig. 8), the complex becomes anhydrous at 70 ° C, the DTA curve (Fig. 8) showing an endothermic region at this temperature. As in the other Cu(II) complexes, the crystallisation nature of the water was confirmed by the RD spectrum of the anhydrous complex after heating at 100 ° C.

In the following step, between 120 and 210 ° C, the deammination of the complex takes place, and then, immediately, the first step of the ligand degradation starts, which corresponds to the loss of the acetamido groups. The DTA curve shows two overlapping peaks in the temperature range

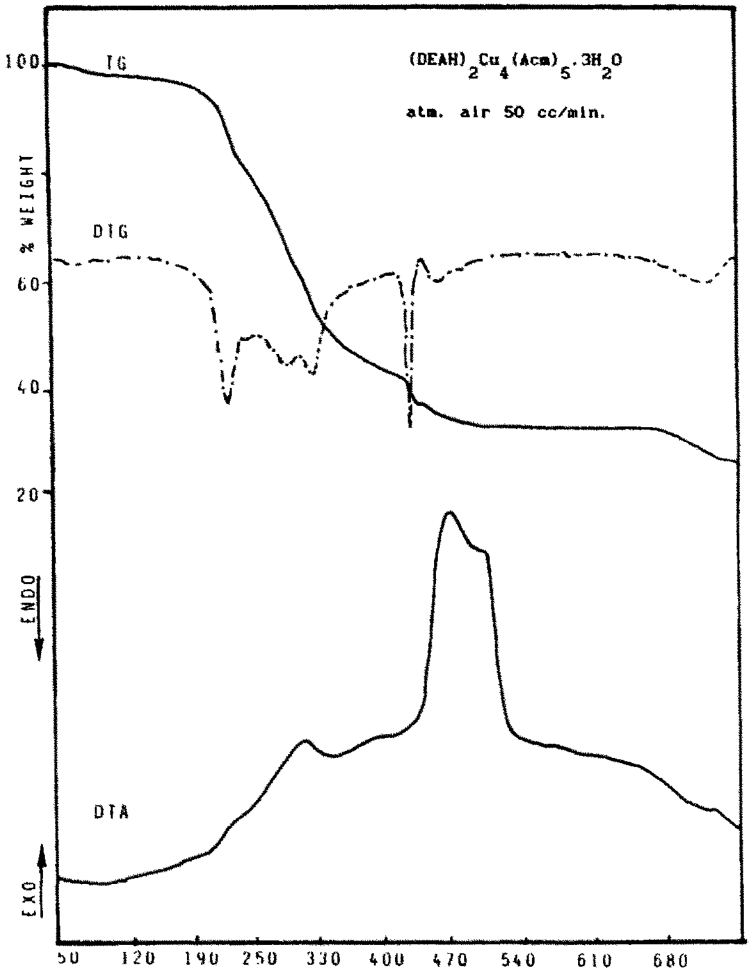

Fig. 7. TG, DTG and DTA thermograms for $(DEAH)_2Cu_4(Acm)_5.3H_2O$ in dynamic air at 10 °C min^{-1}.

270–340 °C: first, an endothermic peak characteristic of deammination; and second, an exothermic peak caused by the first stage of the ligand pyrolysis. The second step in the ligand decomposition sequence corresponds to the loss of the sulphonamido groups. The DTA curve shows the exothermic peak corresponding to this thermal event.

Finally, in all of the above-mentioned Cu complexes, the degradation of the ligand leads to the formation of a Cu thiadiazole derivative [5,8], which, according to experimental results, decomposes to give a mixture of copper oxide and copper sulphate [13]. However, in $(TEAH)_2Cu_4(Acm)_5.3H_2O$, the sulphate is transformed to CuO at about 700 °C, unlike the other two copper complexes whose residues are a mixture of CuO and $CuSO_4$. This is consistent with the IR spectrum of the sample taken at 600 °C which shows

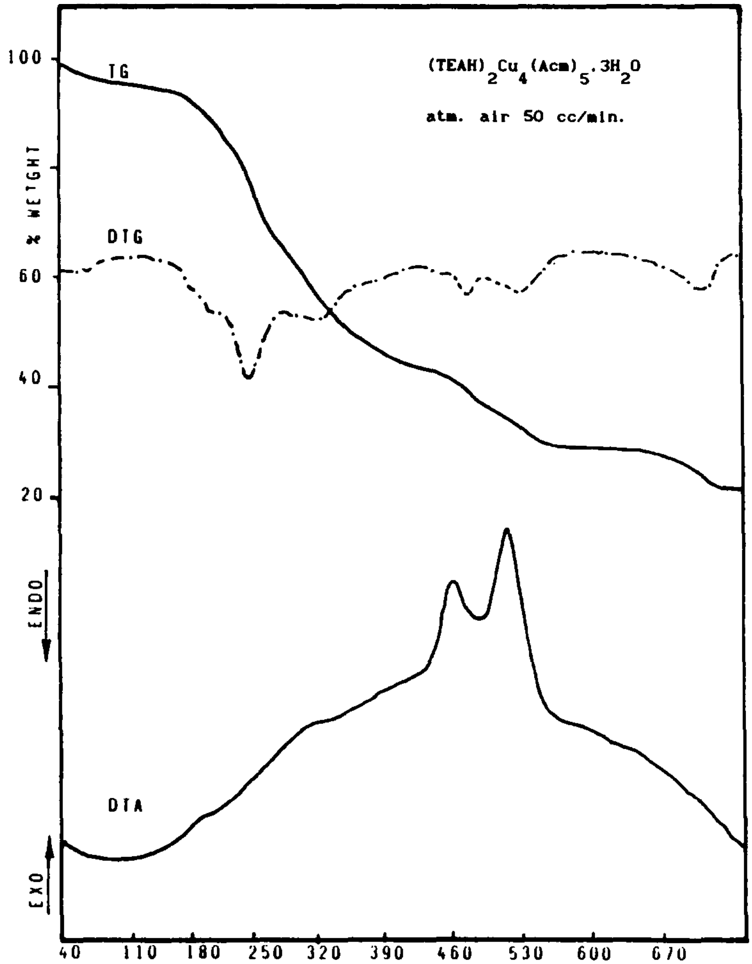

Fig. 8. TG, DTG and DTA thermograms for $(TEAH)_2Cu_4(Acm)_5.3H_2O$ in dynamic air at 10 °C min^{-1}.

bands characteristic of sulphate anion and Cu–O vibration, while the IR spectrum of the solid at 800 °C only exhibits the band corresponding to Cu–O vibration.

The DTA curves exhibit strong exothermic peaks in the temperature range of these proposed oxidation processes.

The thermal reactions of the compounds can be summarised as follows

$$(EAH)_6Cu_2(Acm)_5.H_2O \xrightarrow[\substack{\text{Exp.: } 1.1\% \\ \text{Calc.: } 1.2\%}]{-H_2O} (EAH)_6Cu_2(Acm)_5$$

$$\xrightarrow[\substack{\text{Exp.: } 17.9\% \\ \text{Calc.: } 18.1\%}]{-6EA} Cu_2(Acm)_5 \xrightarrow[\substack{\text{Exp.: } 25.7\% \\ \text{Calc.: } 26.2\%}]{-5SO_2NH_2} Cu_2[Tdz\text{–}AcNH_2]_5$$

$$\xrightarrow[\substack{\text{Exp.: } 18.7\% \\ \text{Calc.: } 19.0\%}]{-5\text{AcNH}_2} \text{Cu}_2[\text{Tdz}]_5 \rightarrow \text{CuO} + \text{CuSO}_4$$

(Residue: exp., 15.5%; calc., 15.6%)

$$(\text{DEAH})_2\text{Cu}_4(\text{Acm})_5.3\text{H}_2\text{O} \xrightarrow[\substack{\text{Exp.: } 2.2\% \\ \text{Calc.: } 2.3\%}]{-2\text{H}_2\text{O}} (\text{DEAH})_2\text{Cu}_4(\text{Acm})_5.\text{H}_2\text{O}$$

$$\xrightarrow[\substack{\text{Exp.: } 11.8\% \\ \text{Calc.: } 10.6\%}]{-\text{H}_2\text{O},\ -2\text{DEA}} \text{Cu}_4(\text{Acm})_5 \xrightarrow[\substack{\text{Exp.: } 43.9\% \\ \text{Calc.: } 44.3\%}]{-5\text{AcNH}_2,\ -5\text{SO}_2\text{NH}_2} \text{Cu}_4[\text{Tdz}]_5$$

$\rightarrow$ 3CuO + CuSO_4 (Residue: exp., 25.6%; calc., 25.5%)

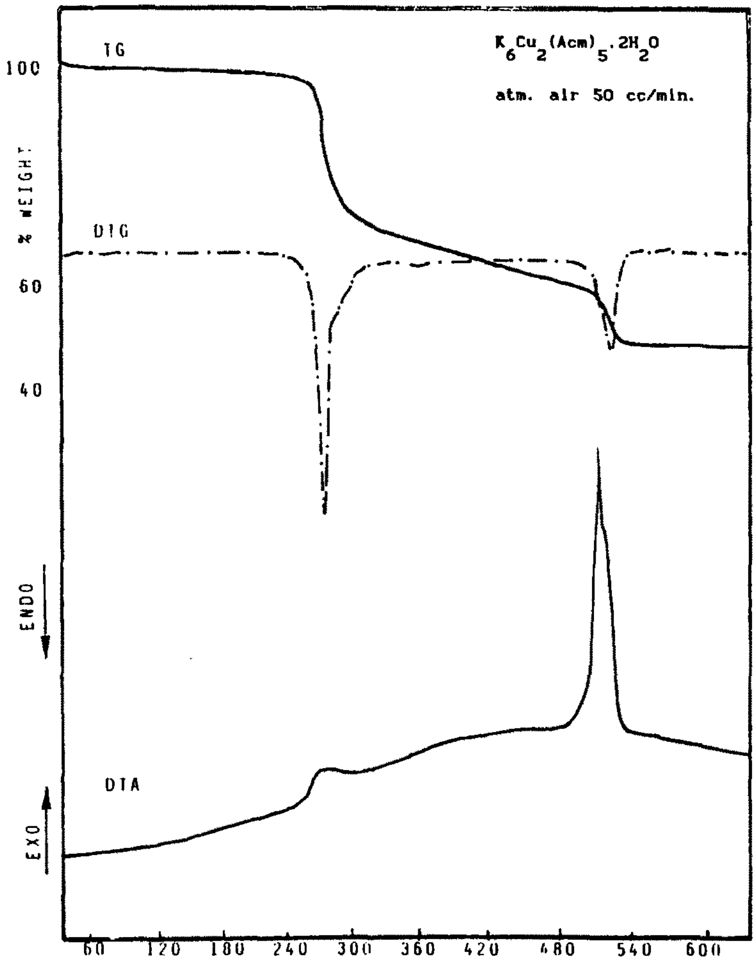

Fig. 9. TG, DTG and DTA thermograms for $K_6Cu_2(Acm)_5.2H_2O$ in dynamic air at 10 °C min^{-1}.

$$(\mathrm{TEAH})_2\mathrm{Cu}_4(\mathrm{Acm})_5.3\mathrm{H}_2\mathrm{O}\ \underset{\text{Calc.: 3.3\%}}{\xrightarrow[\text{Exp.: 3.5\%}]{-3\mathrm{H}_2\mathrm{O}}}\ (\mathrm{TEAH})_2\mathrm{Cu}_4(\mathrm{Acm})_5$$

$$\underset{\text{Calc.: 12.6\%}}{\xrightarrow[\text{Exp.: 12.1\%}]{-2\mathrm{TEAH}}}\ \mathrm{Cu}_4(\mathrm{Acm})_5\ \underset{\text{Calc.: 18.3\%}}{\xrightarrow[\text{Exp.: 18\%}]{-5\mathrm{AcNH}_2}}\ \mathrm{Cu}_4[\mathrm{Tdz{-}SO_2NH_2}]$$

$$\underset{\text{Calc.: 24.7\%}}{\xrightarrow[\text{Exp.: 23.9\%}]{-5\mathrm{SO}_2\mathrm{NH}_2}}\ \mathrm{Cu}_4[\mathrm{Tdz}]_5 \rightarrow \mathrm{CuO} + \mathrm{CuSO}_4 \rightarrow 4\mathrm{CuO}$$

(Residue: exp., 20.1%; calc., 19.8%)

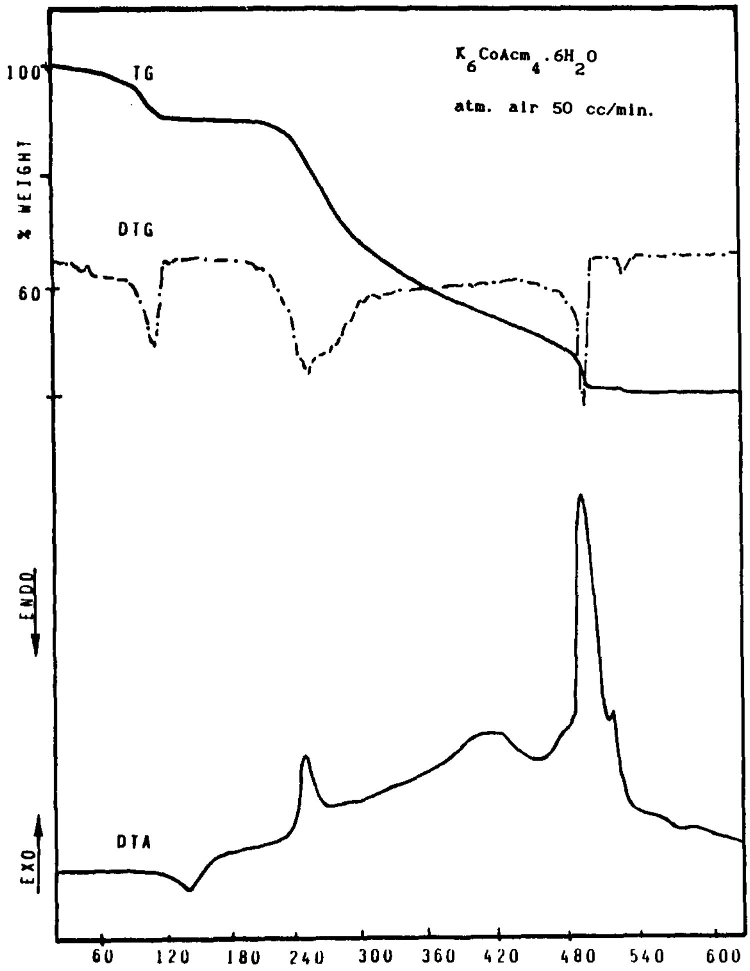

Fig. 10. TG, DTG and DTA thermograms for $K_6Co(Acm)_4.6H_2O$ in dynamic air at 10 °C min^{-1}.

$K_6Cu_2(Acm)_5.2H_2O$ and $K_6Co(Acm)_4.6H_2O$

The TG–DTG curves (Figs. 9 and 10) show that the first weight loss occurs up to 60 °C for $K_6Cu_2(Acm)_5.2H_2O$ and up to 120 °C for $K_6Co(Acm)_4.6H_2O$: this is due to the removal of crystallisation water. The DTA curves (Figs. 9 and 10) exhibit the corresponding endothermic thermal event at the temperature of the dehydration. Then, the Cu(II) and Co(II) anhydrous complexes remain stable up to 260 °C and 230 °C, respectively. The pyrolytic decomposition takes place in a similar way for both compounds in two well-separated steps:

1. A sudden loss in weight, attributed to partial degradation of the ligand,

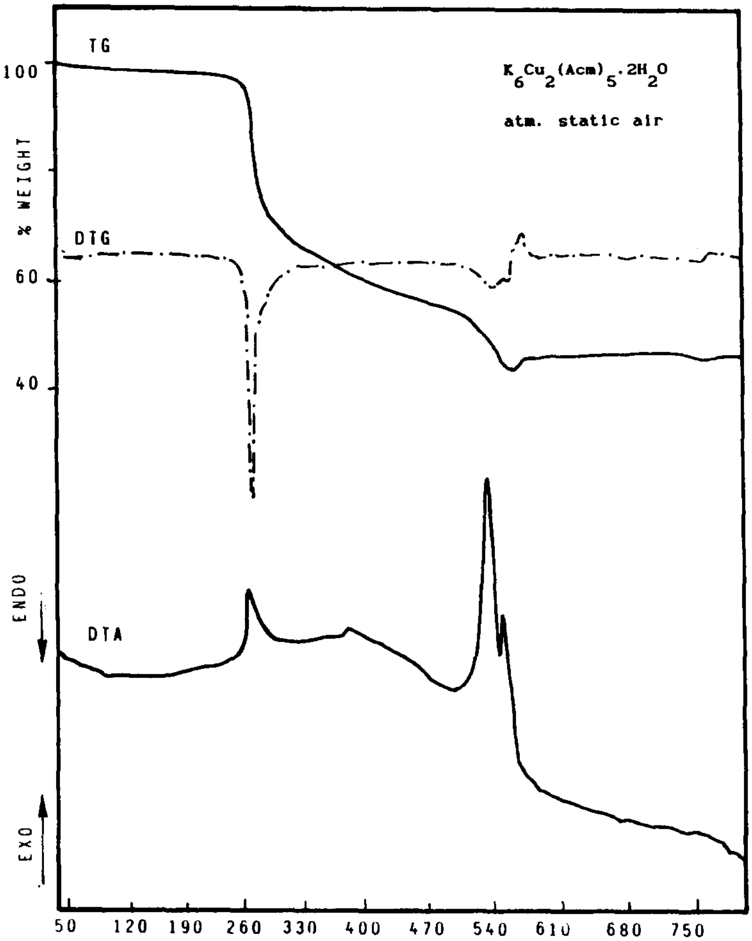

Fig. 11. TG, DTG and DTA thermograms for $K_6Cu_2(Acm)_5.2H_2O$ in static air.

occurs between 260 and 340 °C and between 230 and 300 °C, respectively. The experimental result suggests the formation of a mixture of M(II) thiadiazole derivative and K_2SO_4. Accordingly the IR spectra of the samples taken at 350 °C show a broad band centred over 1400–1500 cm^{-1} and a medium band at 600 cm^{-1}, characteristic of molecules containing S=C=N bonds, and the bands characteristic of the vibrations of sulphate anion. As we reported previously [6], the potassium sulphate would be formed from the sulphonamido moiety.

2. The metal thiadiazole derivative follows the usual scheme of degradation to give MSO_4 and MO.

In the DTA curve of $K_6Cu_2(Acm)_5.2H_2O$, the two steps of ligand

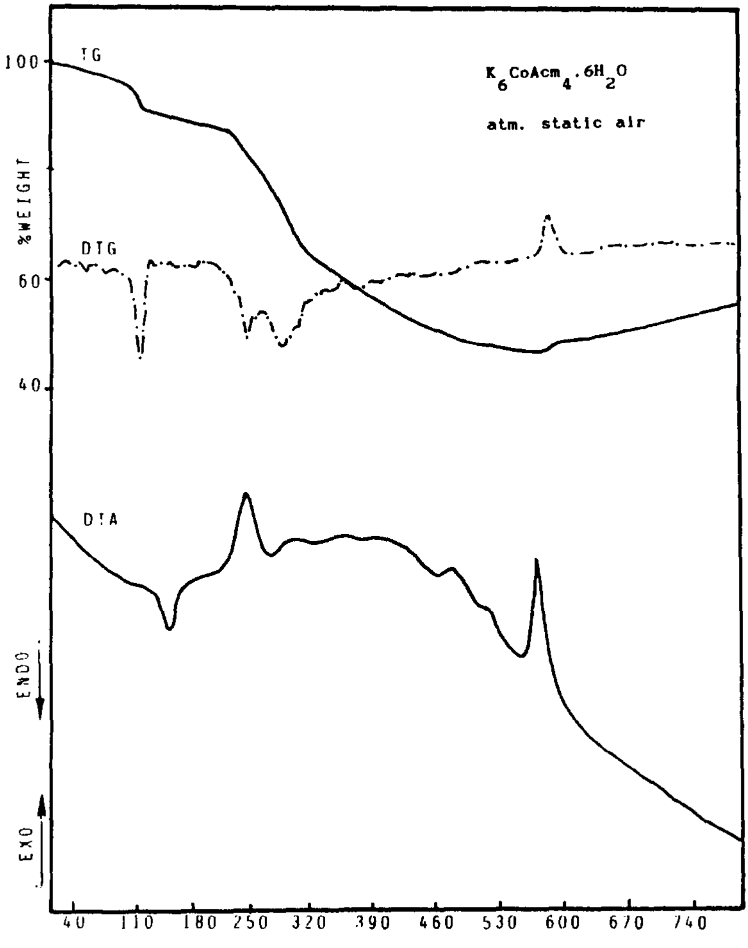

Fig. 12. TG, DTG and DTA thermograms for $K_6Co(Acm)_4.6H_2O$ in static air.

degradation appear as exothermic peaks at 270 and 530 °C. However, the DTA curve of $K_6Co(Acm)_4.6H_2O$ has three exothermic thermal events at 250, 400 and 490 °C, which correspond to the ligand decomposition.

The TG–DTG thermograms of $K_6Cu_2(Acm)_5.2H_2O$ and the $K_6Co(Acm)_4.6H_2O$ were also measured under static air conditions (Figs. 11 and 12). The thermal decomposition is very similar to that in flowing air although there is a small difference in the temperature at which MSO_4 is formed from the S atom of the thiadiazole ring. The TG curve in static air shows more clearly an increase in weight corresponding to the oxidation of MS to MSO_4 and MO.

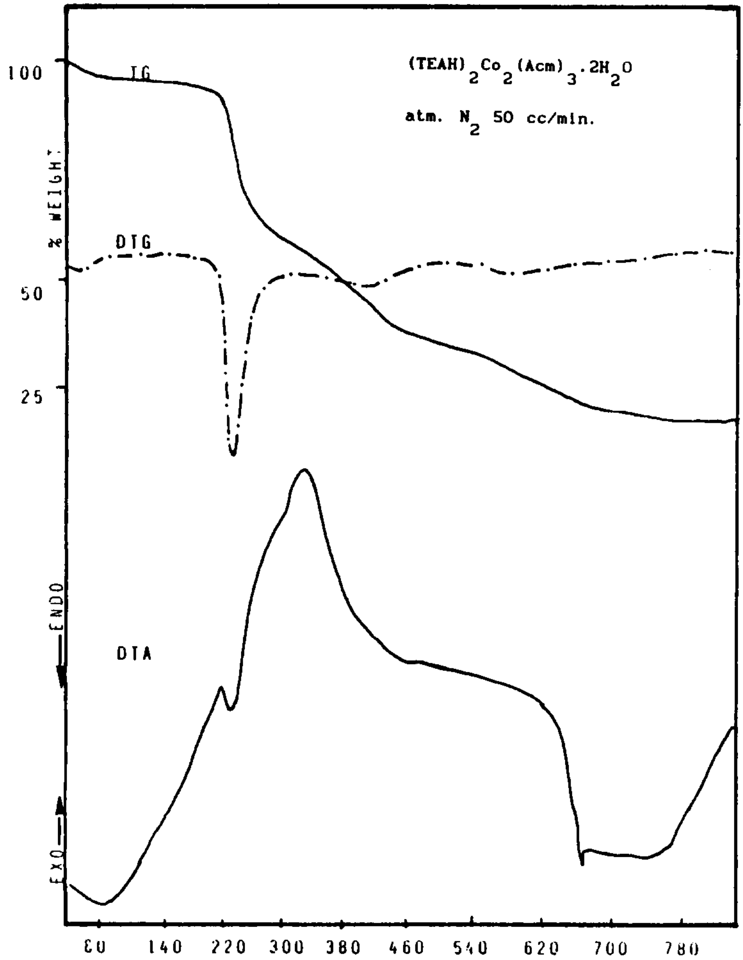

Fig. 13. TG, DTG and DTA thermograms for $(TEAH)_2Co_2(Acm)_3.2H_2O$ in N_2 at 10 °C min^{-1}.

The thermochemical changes observed can thus be represented by the following equations

$$K_6Cu_2(Acm)_5.2H_2O \xrightarrow[\substack{\text{Exp.: 2.1\%}\\ \text{Calc.: 2.4\%}}]{-2H_2O} K_6Cu_2(Acm)_5$$

$$\xrightarrow[\substack{\text{Exp.: 26.8\%}\\ \text{Calc.: 26.3\%}}]{-5\Delta cNH_2} Cu_2[Tdz]_5 + 3K_2SO_4 \rightarrow CuO + CuSO_4 + 3K_2SO_4$$

(Residue: exp., 47.8%; calc., 50.7%)

$$K_6Co(Acm)_4.6H_2O \xrightarrow[\substack{\text{Exp.: 8.9\%}\\ \text{Calc.: 8.4\%}}]{-6H_2O} K_6Co(Acm)_4$$

$$\xrightarrow[\substack{\text{Exp.: 19.4\%}\\ \text{Calc.: 19.6\%}}]{-4\Delta cNH_2} Co[Tdz]_4 + 3K_2SO_4 \rightarrow CoSO_4 + 3K_2SO_4$$

(Residue: exp., 52.4%; calc., 52.8%)

The TG, DTG and DTA curves were also measured in nitrogen atmosphere. The most significant differences between the thermal degradation in flowing air and N_2 are summarised as follows:

1. The residue obtained in N_2 is metal sulphide in all cases. In flowing air, as indicated above, the final product was identified as a mixture of metal sulphate and metal oxide or metal oxide alone.

2. The oxidation process of the thiadiazole derivative which gives MSO_4 and MO, shows a strong exothermic peak in the DTA curve in air which was not observed in N_2.

Figure 13 shows the TG–DTG and DTA curves of the pyrolytic decomposition of $(TEAH)_2Co_2(Acm)_3.2H_2O$ in nitrogen, as an example of the thermal degradation that is typical of all the complexes.

ACKNOWLEDGEMENT

We greatly appreciate financial support from the FAR 88-502 of Spain.

REFERENCES

1 S. Ferrer, A. Jiménez and J. Borrás, Inorg. Chim. Acta, 129 (1987) 103.
2 S. Ferrer, J. Borrás, C. Miratvilles and A. Fuertes, Inog. Chem., 28 (1989) 160.
3 S. Ferrer, J. Borrás, C. Miratvilles and A. Fuertes, Inorg. Chem., 29 (1990) 206.
4 S. Ferrer, G. Alzuet and J. Borrás, J. Inorg. Biochem., 37 (1989) 163.
5 S. Ferrer, J. Borrás, J. Martín-Gil and F.J. Martín-Gil, Thermochim. Acta, 147 (1989) 321.
6 S. Ferrer, J. Borrás, J. Martín-Gil and F.J. Martín-Gil, Thermochim. Acta, 153 (1989) 205.
7 G. Alzuet, S. Ferrer and J. Borrás, J. Inorg. Biochem., 42 (1991) 79.
8 N.B. Singh and J. Singh, J. Inorg. Nucl. Chem., 41 (1979) 1384.
9 L.J. Bellamy, Advances in Infrared Group Frequencies, Vol. II, Chapman and Hall, London, 1968.

10 R.B. Lambert, H.F. Shurvell, L. Verbit, R.G. Cooks and G.H. Strout, Organic Structural Analysis, Macmillan, New York, 1976.

11 M.N. Moreno-Carretero and J.M. Salas Peregrín, J. Therm. Anal., 29 (1984) 1053.

12 M.N. Moreno-Carretero, J.M. Salas Peregrín and A. Mata-Arjona, J. Therm. Anal., 29 (1984) 553.

13 H. Tanaka and N. Koga, J. Chem. Educ., 67 (1990) 612.